

Article

Vallisneria spiralis Promotes P and Fe Retention via Radial Oxygen Loss in Contaminated Sediments

Monia Magri , Sara Benelli  and Marco Bartoli * 

Department of Chemistry, Life Sciences and Environmental Sustainability, University of Parma, 43124 Parma, Italy; monia.magri@unipr.it (M.M.); sara.benelli@unipr.it (S.B.)

* Correspondence: marco.bartoli@unipr.it

Abstract: Microbial respiration determines the accumulation of reduced solutes and negative redox potential in organic sediments, favoring the mobilization of dissolved inorganic phosphorus (DIP), generally coprecipitated with Fe oxyhydroxides. Macrophytes releasing oxygen from the roots can contrast DIP mobility via the oxidation of anaerobic metabolism end-products. In this work, the submerged macrophyte *Vallisneria spiralis* was transplanted into laboratory microcosms containing sieved and homogenized organic sediments collected from a contaminated wetland. Sediments with and without plants were incubated under light and dark conditions for oxygen and DIP fluxes measurements and pore water characterization (pH, oxidation-reduction potential, DIP, dissolved Mn, and Fe). Bare sediments were net DIP sources whereas sediments with *V. spiralis* were weak DIP sources in the dark and large sinks in light. *V. spiralis* radial oxygen loss led to less negative redox potential and lower Fe, Mn, and DIP concentrations in pore water. Roots were coated by reddish plaques with large amounts of Fe, Mn, and P, exceeding internal content. The results demonstrated that at laboratory scale, the transplant of *V. spiralis* into polluted organic sediments, mitigates the mobility of DIP and metals through both direct and indirect effects. This, in turn, may favor sediment colonization by less-tolerant aquatic plants. Further in situ investigations, coupled with economic analyses, can evaluate this potential application as a nature-based solution to contrast eutrophication.

Keywords: organic sediments; restoration; submerged macrophytes; roots; nature-based solutions



Citation: Magri, M.; Benelli, S.; Bartoli, M. *Vallisneria spiralis* Promotes P and Fe Retention via Radial Oxygen Loss in Contaminated Sediments. *Water* **2023**, *15*, 4222. <https://doi.org/10.3390/w15244222>

Academic Editor: Danny D. Reible

Received: 30 October 2023

Revised: 28 November 2023

Accepted: 5 December 2023

Published: 7 December 2023



Copyright: © 2023 by the authors. Licensee MDPI, Basel, Switzerland. This article is an open access article distributed under the terms and conditions of the Creative Commons Attribution (CC BY) license (<https://creativecommons.org/licenses/by/4.0/>).

1. Introduction

Eutrophication is a degenerative process of inland aquatic ecosystems resulting from an excess availability of dissolved inorganic nutrients that generally limit algal and plant growth [1]. Nutrient availability stimulates the production of biomass from autotrophs, often in excess of the mineralization capacity of heterotrophs and to the oxygen (O_2) available in water [2]. This degenerative process determines two main effects: the net accumulation of organic matter in sediments and the build-up of anaerobic metabolism end-products in pore waters when O_2 is depleted [3]. The latter is favored by the low solubility of this molecule, by the evasion to the atmosphere of the O_2 produced by plants in excess of solubility thresholds, and by the large demand and consumption of electron acceptors for organic carbon mineralization [4]. Eutrophication can be contrasted effectively by reducing external nutrient loads, by acting at the origin of the problem [5,6]. However, such action can produce little evidence of decreasing rates of primary production due to internal recycling [7,8]. Indeed, the accumulation of organic matter in the benthic compartment may fuel mechanisms of nutrient recycling that more than compensate for the reduction of external loads and maintain for decades algal blooms and large photosynthetic rates [9]. The reduction of internal nutrient recycling is, therefore, another important action to contrast eutrophication [10].

At present, the restoration technologies of eutrophic water mainly include physical, chemical, and ecological methods [11]. Physical (e.g., sediment dredging) and chemical (e.g.,

use of sorbent material) methods have often been used to treat emergency water pollution, but in situ applications have proven to be costly, and the effects weakened over time [12] or reversed due to changing environmental conditions [13]. The ecological methods represent an important alternative, and with this respect, the transplant of macrophytes in shallow organic sediments represents the most economical and effective option [11,14]. Macrophytes tend to die and disappear in organic sediments due to the accumulation of phytotoxic compounds in pore water or due to increased turbidity of the water column limiting light penetration [15–18]. In shallow ecosystems where light is available but sediments are loaded with organic matter, not all the species of macrophytes are suitable for transplant actions. Indeed, even extremely small variations (e.g., 0.2%) of the organic matter content in sediment are reported to inhibit the growth of low tolerant macrophytes [19]. The latter have not evolved adaptations to counteract chemically reduced conditions in sediments [20–22]. However, there are macrophytes characterized by elevated plasticity, with a large capacity to release part of the photosynthetically produced O₂ to the rhizosphere [23]. Macrophytes displaying high rates of radial oxygen loss (ROL) not only allow root cells respiration within a strictly anoxic medium but release to the rhizosphere an electron acceptor that can oxidize chemically reduced compounds, directly or through microbes [24–26]. Such plants can, therefore, reduce the toxicity of sediments and contribute via various mechanisms, including uptake or precipitation, to the reduction of internal nutrient regeneration [27–29]. As well as these biogeochemical services, the development of macrophyte meadows is demonstrated to provide many other ecosystem services [30,31].

Vallisneria spiralis (Hydrocharitaceae) is a perennial, mostly stoloniferous submersed macrophyte that provides to aquatic ecosystems different biogeochemical services [32]. This plant can grow in organic, heavily contaminated substratum [33–36] and has a demonstrated capacity to release variable O₂ amounts to sediments, depending on the season (i.e., larger amounts during summer, when heterotrophic microbial activity is higher) or on the sedimentary organic content (i.e., larger amounts along organic matter sedimentary gradients) [37,38]. The effects produced by *V. spiralis* on benthic biogeochemistry addressed mostly nitrogen removal via denitrification in fluvial sediments [33,39,40], whereas the effects of this macrophyte on phosphorus benthic cycling in organic contaminated sediments were comparatively poorly investigated [41]. Rooted macrophytes may promote phosphorus retention both directly through root uptake and indirectly through the reoxidation of redox-sensitive compounds, which can bind or co-precipitate phosphorus [42].

In this work, individuals of *V. spiralis* were transplanted in reconstructed microcosms containing organic sediments collected from a contaminated wetland area in northern Italy. The main aim of the work was to understand the effects of *V. spiralis* transplant on mitigation of phosphorus and phosphorus-associated metals (iron and manganese) recycling. Microcosms with bare sediments and with sediments transplanted with *V. spiralis* were conditioned for 3 weeks in large aquaria to check whether the macrophyte was growing and to allow the development of steady chemical gradients and stable microbial communities in the two treatments [43]. Bare and vegetated sediments were incubated in the light and in the dark to measure net fluxes of O₂ and dissolved inorganic phosphorus (DIP) and then characterized for different pore water features. At the end of the experiment, the roots of *V. spiralis* were analyzed for the amount of Fe, Mn, and P immobilized on their plaques and inside their biomass, in order to speculate about the direct (i.e., uptake) and indirect (i.e., via ROL) effects of the macrophyte on DIP retention.

It was hypothesized that: (1) *V. spiralis*, through its plasticity, can adapt and survive in organic sediments likely due to increased release of O₂ to the rhizosphere, at the expense of the O₂ evolved to the water column; (2) the large amounts of O₂ diffusing to the sediments from the roots can oxidize and precipitate Fe²⁺ and Mn²⁺ dissolved in pore water and form plaques on the root surface that in turn co-precipitate DIP; (3) the amount of DIP precipitated on the roots surface exceeds the amount present in the roots biomass, suggesting that indirect DIP retention mechanisms promoted by the plant should be considered to be a biogeochemical service as direct DIP uptake. These issues are discussed

with two main perspectives: the potential use of macrophytes as nature-based solutions to contrast eutrophication and internal DIP recycling and the negative consequences of macrophyte removal, a common practice in irrigation and drainage canals as well as in the littoral zone of many lakes, for sediment biogeochemistry and water quality.

2. Materials and Methods

2.1. Sediment, Plants and Water Sampling and Microcosms Setup

Sediments were collected in early March 2022 from the central part of a shallow wetland area (Vallazza, Mantua, Italy, $45^{\circ}08'00''$ N $10^{\circ}48'43''$ E) within the Mincio River fluvial system. The Vallazza wetland is contaminated by the discharge of the wastewater treatment plant of the town of Mantua (100,000 Population Equivalent) and by organic microcontaminants from a chemical plant. For its level of contamination, the Vallazza wetland is within the list of SINs (polluted Site of National Importance), regularly monitored by the Italian Institute for Environmental Protection and Research. The water column at the Vallazza sampling site was 1 m deep. Surface sediments (0–10 cm horizon, nearly 30 L) were collected in transparent plexiglass liners by a hand corer, transferred into a 40 L tank, and brought to the laboratory. Individuals of *V. spiralis* ($n = 60$) were collected upstream of the Vallazza wetland, from a marginal area of the Mincio River with organic sediments (9% as loss on ignition), where plants were collected for other previous experiments [39]. Plants were collected by hand so as not to damage the rhizosphere and were selected to be similar in size. The sediment adjacent to the roots was gently washed out in situ, and epiphytic organisms and snails, when present, were gently removed from the leaves by hand. Plants were transported to the laboratory submersed in a 50 L tank provided with aeration. Nearly 300 L of water was finally collected from the Mincio River upstream of the Vallazza wetland area, brought to the lab, and used for preincubation and incubation procedures. In the laboratory, the sediment was sieved (1 mm mesh size) to remove large debris, homogenized, and transferred into a tank where it was left for a few days, after which the overlying water was siphoned off. No macrofauna was found during sieving.

Cylindrical Plexiglass microcosms (outer diameter 8 cm, height 10 cm, $n = 22$) were filled with the homogenate sediment (Figure 1a). Microcosms were then covered with aluminum foil to keep sediments in darkness. In half of the microcosms, 2 individuals of *V. spiralis* were transplanted. All microcosms were then transferred into a 100 L aquarium containing water from the Mincio River and placed in a temperature-controlled room. The microcosms were exposed to environmental conditions mimicking those observed in situ in March, with a water temperature of 18°C and a 12/12-h light-dark photoperiod. Halogen lamps were placed above the aquarium, and illumination was set at $250 \mu\text{E m}^{-2}$ to reproduce the average light intensity during spring in northern Italy. The preincubation period lasted 3 weeks. This period was considered to be sufficient for the plant to overcome transplant stress and promote its growth and for the bacterial community to recover and reach the steady-state conditions after sediment sieving, homogenization, and plant transplant [43]. The water in the aquarium was gently mixed by pumps, avoiding sediment resuspension, and dissolved O_2 was maintained at saturation, as measured in situ, by constant air bubbling. Nearly 20% of the water in the aquarium was replaced with in situ water every 3 days.

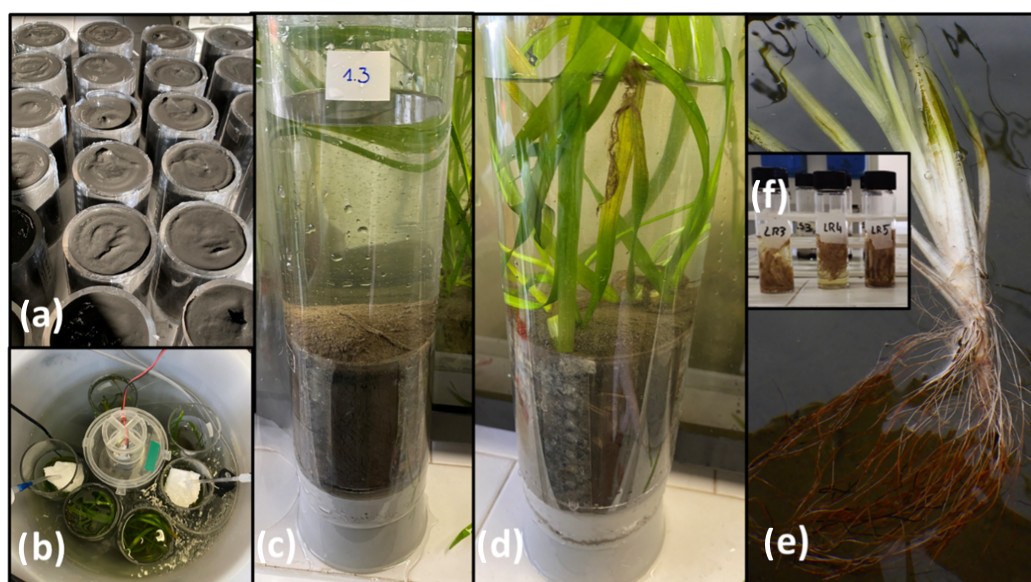


Figure 1. Microcosm setup and components for sediment study: (a) Preparation of the cylindrical microcosms with the contaminated sediment homogenate; (b) an incubation tank for flux measurements; (c) a detailed view of a transparent Plexiglass liner containing a bare sediment microcosm; (d) a microcosm with sediment + *V. spiralis*; (e) iron-coated roots of the macrophyte at the end of the experiment; (f) acid dissolution of the iron coating from roots.

2.2. Light-Dark Incubations

After the preincubation period, sets of paired light and dark incubations were repeated three times (on 25 March 2022, 27 March 2022, and 30 March 2022). For each incubation set, six microcosms were randomly collected from each treatment: bare sediment (S) and sediment with *V. spiralis* (S + V). They were then transferred underwater into cylindrical Plexiglass liners perfectly fitting their size (inner diameter 8 cm, height 30 cm) closed at the bottom by a rubber stopper (Figure 1c,d). Each liner, equipped with a Teflon-coated magnet positioned in the upper part, was placed into two incubation tanks, one for each treatment (Figure 1b). During incubations, the magnet rotated at 40 rpm and was driven by a central motor to mix and homogenize the water column, preventing sediment resuspension. In vegetated microcosms, a plastic net prevented *V. spiralis* leaves to interfere with the rotating magnets. Two subsequent incubations were carried out, the first under dark and the second under light conditions. For light incubation, a halogen lamp was placed above the tanks, maintaining light intensity at $250 \mu\text{E m}^{-2}$, as during the preincubation phase. After dark and light incubations, microcosms were transferred from the incubation tank to the aquarium.

Light and dark incubations were short-term and lasted 3 h to keep O_2 concentration within 20% of initial values and started when transparent floating lids were positioned on the top of the cores [44]. Initial and final water samples were collected from each core with plastic syringes and transferred into 12 mL glass vials (Exetainer, Labco, High Wycombe, UK) for O_2 determination through iodometric titration using the Winkler method [45] and to 10 mL glass vials for the immediate spectrophotometric determination of DIP [46]. The subsamples for DIP analyses were filtered through 0.7 μm glass fiber filters. Oxygen and DIP fluxes were calculated with the equation

$$F_x = \frac{(C_f - C_i)V}{At} \quad (1)$$

where F_x is the flux of the solute X (O_2 or DIP, $\mu\text{mol m}^{-2} \text{h}^{-1}$), C_f and C_i are the final and the initial concentration of X (μM), V is the volume of the water overlying sediments (L), A is the sediment surface (m^2) and t is the incubation time (h).

2.3. Sediment and Pore Water Feature Analyses

After the third sequential incubation, microcosms were separated from liners to analyze sedimentary features. Oxygen microprofiles were measured with a polarographic microsensor (50 μm tip, Unisense, Aarhus, Denmark) mounted on a manual manipulator (Tesa Hite, 300, CH) and connected to an amperometer (PA2000, Unisense, DK). Profiles were measured in the darkness in 6 different microcosms per treatment, maintained submerged in aerated water. Diffusive oxygen uptake rates (DOU) were calculated from the measured O_2 microprofiles as described in [47], assuming zero-order consumption kinetics and thus homogeneous respiration within the oxic sediment layer [48]. This assumption seems reasonable for microcosms containing reconstructed, homogenized organic sediments. For this purpose, a second-order polynomial function was fitted to all oxygen profiles, and concentration gradients were calculated according to [49]. The pH and redox potential were measured in randomly chosen bare and vegetated microcosms ($n = 6$) with combined pH and platinum electrodes (Hamilton) connected to an mV meter (Beckman Coulter, Brea, USA), inserting the electrodes in the central part of the microcosm at 3–5 cm depth in sediments. Pore water was extracted from another set of 6 bare and vegetated microcosms by vertically inserting Rhizon samplers in the central part of the microcosms to collect an integrated pore water sample along the 0–5 cm sediment horizon. A subsample of the collected pore water was immediately acidified with 100 μL of concentrated HNO_3 for the analyses of dissolved metals (Fe^{2+} , Mn^{2+}) via atomic absorption (Varian AA280 FS) whereas another subsample was transferred into a glass vial for immediate spectrophotometric DIP analysis. Sediment aliquots (10 mL, along the vertical profile) were subsampled via cut-off plastic syringes to analyze density, porosity, water content after desiccation at 60 °C until constant weight, and organic matter content (%) as loss on ignition (LOI) after incineration in muffle furnace at 450 °C.

2.4. Root Analyses

At the end of flux and pore water measurements, plants were gently retrieved from the microcosms, and the below and above-ground portions were separated. Roots were gently rinsed with deionized water to remove sediment particles, and subsamples of root hair ($n = 10$), randomly collected from different plants, were submersed in 40 mL glass vials filled with 20 mL of 0.5 M HCl (Figure 1e,f). The roots, submersed in acid, were maintained at room temperature (25 °C) and placed on an orbital shaker for 16 h [50]. During the treatment, the color of the root hair shifted from reddish to white, and the color of the acid solution shifted from transparent to yellowish. The roots were then removed from the HCl solution that was diluted with distilled water and analyzed for DIP and dissolved Mn^{2+} and Fe^{2+} as previously described. After the HCl treatment, roots were rinsed with deionized water, dried at 60 °C until constant weight, weighed, and incinerated. The incinerated roots have been ground, suspended in glass vials filled with 10 mL of 1 M HCl, and placed on an orbital shaker for 16 h at room temperature. The solution was then centrifuged, and the supernatant was diluted and analyzed to determine the concentration of total P (spectrophotometry, [51]) and total Fe and Mn as previously described. The two described methods allowed the splitting of the total amount of P, Fe, and Mn associated with the macrophyte roots into the amount coating the root surface and the amount within the root biomass.

2.5. Statistical Analyses

Oxygen microprofiles measured in bare and vegetated sediments were compared via a *t*-test. A three-way ANOVA was performed to test differences among the three incubation days and between conditions (light and dark) and treatments (bare sediment and sediment with *V. spiralis*). Differences in pore water features between treatments were tested via a one-way ANOVA. The significance was set at $p < 0.05$. Analyses and graphs were performed with Sigma Plot (Version 15.0).

3. Results and Discussion

3.1. Sedimentary Features and Macrophytes Plasticity

The sediment at the study site was fluffy and black, releasing large amounts of methane (CH_4) via ebullition. It displayed a homogeneous dark color and structure along the vertical profile and had no evidence of stratification or bioturbation by macrofauna. This superficial layer had a water content of $80.1 \pm 0.5\%$, a density of $1.07 \pm 0.03 \text{ g cm}^{-3}$, and a porosity of 0.86 ± 0.02 . The organic matter content was $17.5 \pm 1.8\%$. Such a percentage is nearly two-fold higher than that reported for riparian fluvial wetlands upstream the study site where *V. spiralis* biogeochemical ecosystem services were experimentally quantified (i.e., $6\% < \text{OM} < 10\%$ [39,40,52]). Results from previous studies by [38–40,52] suggest that *V. spiralis* can modulate ROL depending on the season and the organic matter content of the substratum, increasing the amount of photosynthetically produced O_2 delivered to the roots during warmer as compared to colder months and in organic as compared to mineral sediments. Such a strategy represents an adaptation of the macrophyte to cope with changing pore water chemistry in sediments during summer when microbial respiration increases and phytotoxic anaerobic metabolism end-products accumulate in the pore water. A similar build-up of phytotoxic solutes in the pore water, coupled with chemically reduced conditions, also occurs along gradients of organic matter content in sediments [33]. It can be speculated that to survive in sediments with 17% OM content, transplanted *V. spiralis* individuals need to maximize O_2 delivery to the rhizosphere that was previously estimated to vary between 6 (winter) and $164 \mu\text{mol O}_2 \text{ g}_{\text{dw}}\text{root}^{-1}\text{h}^{-1}$ (late summer) [38]. Such adaptation would result in a decreased oxygenation of the water column and large oxidation of the pore water, as an important fraction of the O_2 produced by the plant is transferred to the sediment. Other forms of plasticity are very different from that of *V. spiralis*. Indeed, the literature reports for *Potamogeton perfoliatus* and other macrophytes a summer reduction of ROL due to decreased permeability of roots, minimizing O_2 losses and contrasting the diffusion of phytotoxic solutes within the plant tissues [53–55].

3.2. Oxygen Profiles and Diffusive O_2 Uptake in Bare and Vegetated Sediments

After the 3-week conditioning period, O_2 microprofiles were carried out in microcosms with sediment bare (S) and in sediment with *V. spiralis* (S + V) ($n = 6$ per treatment) revealed significantly different O_2 penetration depth (OPD) in the two treatments (t -test, $t = -14.025$, $DF = 10$, $p < 0.001$) (Figure 2). OPD averaged $3.0 \pm 0.1 \text{ mm}$ in bare sediments and $4.4 \pm 0.2 \text{ mm}$ in sediments with the macrophyte. The diffusive O_2 consumption in bare and vegetated sediments was determined per unit area by integrating the O_2 consumption rates per unit volume of sediment over the OPD [48]. The combination of higher concentration gradients but lower OPD in treatment S and of lower concentration gradient but higher OPD in treatment S + V resulted in not statistically different DOUs, averaging 898 ± 197 and $816 \pm 212 \mu\text{mol O}_2 \text{ m}^{-2} \text{ h}^{-1}$ in S and S + V, respectively (t -test, $t = 1.46$, $DF = 10$, $p = 0.174$) (Figure 2). Oxygen profiles were limited to the upper layer of sediment in the microcosms and did not investigate the rhizosphere. A previous study has demonstrated via planar optodes that *V. spiralis* releases O_2 from the roots to the sediments and creates micro oxic zones adjacent to the roots, both during the day and during the night [37]. The profiles carried out in this experiment revealed higher O_2 penetration depth in the sediment with *V. spiralis*. Such difference is likely due to the subsurface oxidation of reduced solutes by the plant ROL, decreasing the request of electron acceptors and the redox gradients along the sediment profile, as during microprofiling bottom water O_2 concentration was comparable in S and S + V. Different studies in the literature have addressed the role of aquatic plants in modulating sediment redox and diffusive O_2 uptake, reporting contrasting results that depend on different rates of ROL by emergent and submersed plants [56,57]. Results from this study suggest that *V. spiralis* increases O_2 penetration in sediments but does not affect DOU.

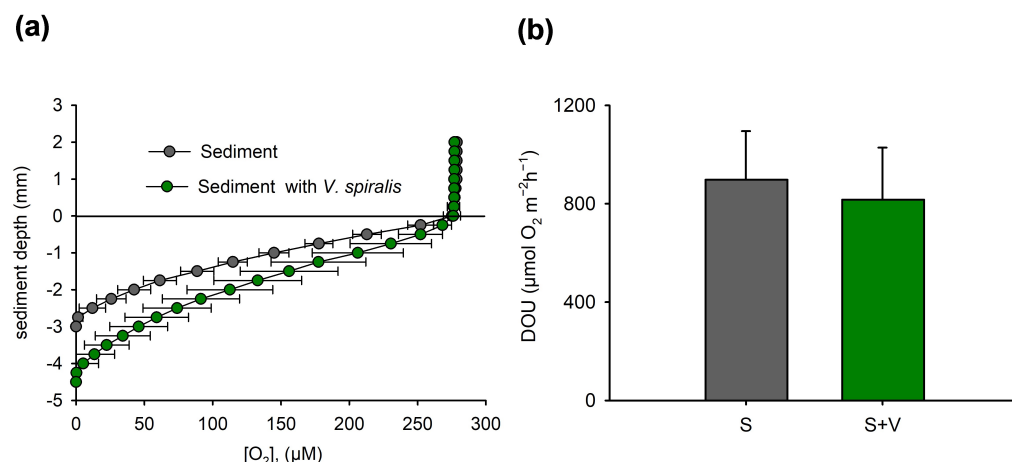


Figure 2. Oxygen microprofiles and diffusive uptake in sediment microcosms: (a) O_2 microprofiles carried out in microcosms containing bare sediment (S) and sediment with *V. spiralis* (S + V); (b) Diffusive O_2 uptake calculated from the microprofiles for the two treatments.

3.3. Net O_2 and DIP Fluxes Measured in the Light and the Dark

During the 3-week preincubation period *V. spiralis* grew in the microcosms, with stolons producing 1 or 2 new plants in each microcosm. The total average biomass of transplanted *V. spiralis* individuals in the microcosms was quantified at the end of the experiment in $70.8 \pm 8.5 \text{ g}_{\text{dw}} \text{ m}^{-2}$ (average \pm standard deviation, $n = 11$). A major fraction of the total biomass was allocated in fronds ($57.9 \pm 7.8 \text{ g}_{\text{dw}} \text{ m}^{-2}$) whereas root biomass represented 18% of the total ($12.9 \pm 3.3 \text{ g}_{\text{dw}} \text{ m}^{-2}$). The three-way analysis of variance on dissolved O_2 fluxes suggests that results from measurements performed on different days were similar whereas there were significant differences between treatments (i.e., S and S + V) and incubation conditions (i.e., light versus dark fluxes, but only in sediment with *V. spiralis*) (Table 1 and Figure 3). Bare sediments always acted as a net O_2 sink in the dark and light incubations, with an average O_2 uptake of $792 \pm 57 \mu\text{mol m}^{-2} \text{ h}^{-1}$ (pooled data for the three incubation days and the two incubation conditions, $n = 36$). Dark O_2 consumption in vegetated sediments was nearly 3.5-fold higher than that in bare sediments and averaged $2940 \pm 177 \mu\text{mol m}^{-2} \text{ h}^{-1}$ (pooled data for dark incubations of S + V, $n = 18$). Photosynthetic O_2 production to the water column by *V. spiralis* balanced sediment respiration resulting in rates of net ecosystem metabolism (NEM) not significantly different from zero ($-27 \pm 69 \mu\text{mol m}^{-2} \text{ h}^{-1}$, pooled data for light incubations of S + V, $n = 18$) and in comparable absolute values of respiration (R) and gross primary production (GPP) rates (Figure 3).

Assuming a conservative value of ROL in the light of $39 \pm 16 \mu\text{mol O}_2 \text{ g}_{\text{dw}} \text{ root}^{-1} \text{ h}^{-1}$ [38] a minimum amount of O_2 delivered by *V. spiralis* to the sediment in this experiment can be estimated at $510 \pm 306 \mu\text{mol O}_2 \text{ m}^{-2} \text{ h}^{-1}$. This value likely underestimates the true ROL in the contaminated sediment of the Vallazza wetland due to the much larger organic matter content in the latter as compared to the sediments analyzed by [38]. Moreover, after the 3-week preincubation period, all vegetated microcosms had 1 or 2 new plants, suggesting a net growth of *V. spiralis* (i.e., a positive daily O_2 budget). As rates of net ecosystem metabolism measured in the light and reported in Figure 3 equal net primary production by *V. spiralis* plus sediment respiration and as the true net primary production by *V. spiralis* includes the fraction released to the water column and the fraction released to the sediment (ROL), it is possible from the measured fluxes and from the data reported in the literature to reconstruct O_2 dynamics in the S + V treatment (Figure 4). The ratio between the calculated true NPP by *V. spiralis* ($1299 \pm 390 \mu\text{mol O}_2 \text{ m}^{-2} \text{ h}^{-1}$) and the molar C:P stoichiometry of the plant (nearly 100, [39]) allows the estimation of a minimum theoretical net assimilation of DIP by the macrophyte of $13 \pm 4 \mu\text{mol DIP m}^{-2} \text{ h}^{-1}$.

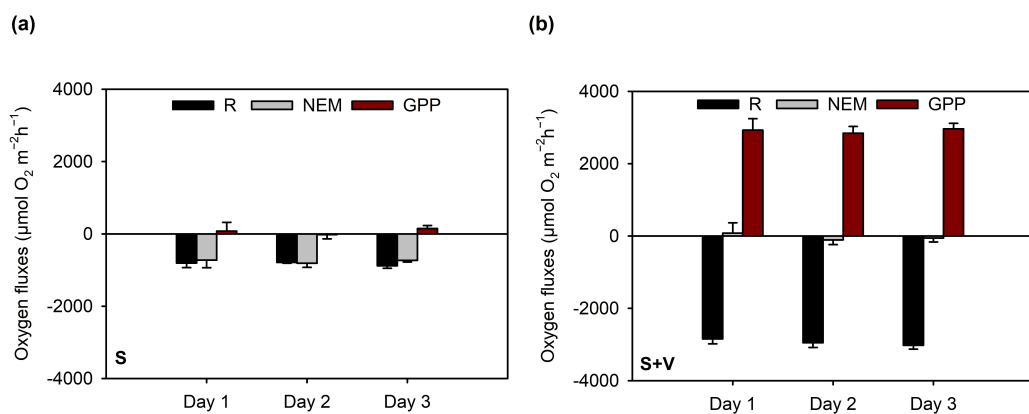


Figure 3. Rates of measured dark respiration (R) and net ecosystem metabolism (NEM) and of calculated gross primary production (GPP=NEM-R) in reconstructed microcosms containing bare sediment (S) (a) and bare sediment with transplanted individuals of *V. spiralis* (S + V) (b). Light and dark incubations were carried out over 3 different days after a 3-week conditioning period. Averages \pm standard errors ($n = 6$) are reported.

Table 1. Three-way analysis of variance of dissolved O_2 and inorganic phosphorus fluxes measured on 3 different days in the light and in the dark in microcosms with bare sediment (S) and with sediment and *V. spiralis* (S + V). Significant values are printed in bold.

Parameter	Source of Variation	DF	SS	MS	F	p
O_2 fluxes	Treatment (S vs. S + V)	1	8,625,871.36	8,625,871.36	72.83	<0.001
	Condition (D vs. L)	1	40,040,426.36	40,040,426.36	338.06	<0.001
	Time (D1 vs. D2 vs. D3)	2	144,181.34	72,090.67	0.61	0.547
	Treat. \times Condit.	1	36,375,693.71	36,375,693.71	307.12	<0.001
	Treat. \times Time	2	54,762.21	27,381.10	0.23	0.794
	Condit. \times Time	2	63,928.11	31,964.05	0.27	0.764
	Treat. \times Condit. \times Time	2	1722.28	861.14	0.007	0.993
	Residual	60	7,106,348.76	118,439.14		
	Total	71	92,412,934.15	1,301,590.62		
DIP fluxes	Treatment (S vs. S + V)	1	1633.11	1633.11	182.96	<0.001
	Condition (D vs. L)	1	509.97	509.97	57.13	<0.001
	Time (D1 vs. D2 vs. D3)	2	3.19	1.59	0.18	0.837
	Treat. \times Condit.	1	342.94	342.94	38.42	<0.001
	Treat. \times Time	2	8.12	4.06	0.45	0.637
	Condit. \times Time	2	16.70	8.35	0.93	0.398
	Treat. \times Condit. \times Time	2	7.21	3.60	0.40	0.669
	Residual	60	535.54	8.92		
	Total	71	3056.81	43.05		

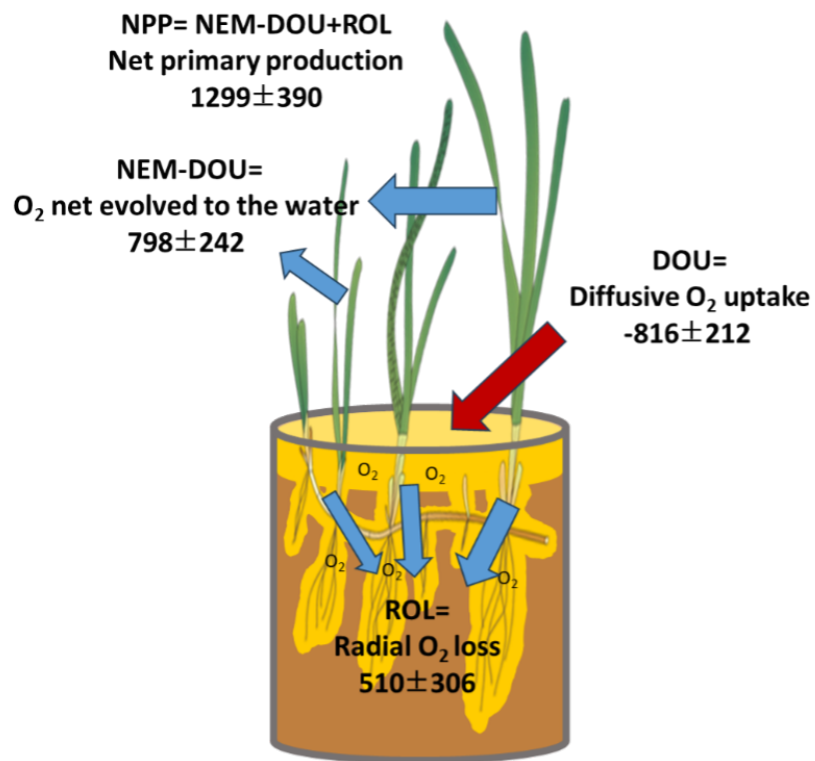


Figure 4. Reconstructed O_2 fluxes in the light in the S + V treatment. The O_2 net evolved to the water can be quantified by combining NEM, reported in Figure 3, with DOU, reported in Figure 2. The *true* net primary production by the macrophyte can be estimated by adding to the calculated amount of O_2 released to the water column by *V. spiralis* the estimated ROL. The reported net primary production rate of 1299 ± 390 is considered a minimum value as ROL was taken from a study carried out in sediments with lower OM content as compared to the Vallazza wetland. All units are $\mu\text{mol } O_2 \text{ m}^{-2} \text{ h}^{-1}$.

The three-way analysis of variance on DIP fluxes suggests that also, for this solute, the factor time was not significant (Table 1). In treatment S, DIP fluxes were always positive (from the sediment to the water column) and not statistically different in the light and dark incubations (Table 1 and Figure 5). They averaged $7.5 \pm 1.0 \mu\text{mol m}^{-2} \text{ h}^{-1}$ (pooled data for the 3 incubation days and the two incubation conditions, $n = 36$). Sediments with *V. spiralis* regenerated in the dark significantly lower amounts of DIP to the water column as compared to treatment S ($2.3 \pm 1.2 \mu\text{mol m}^{-2} \text{ h}^{-1}$, Figure 5) whereas in the light they were net DIP sinks with an uptake averaging $7.3 \pm 1.7 \mu\text{mol m}^{-2} \text{ h}^{-1}$ (pooled data for the 3 light incubations, $n = 18$). The comparison between theoretical net DIP uptake calculated from O_2 fluxes and DIP fluxes measured in light incubations in the S + V treatment (approximately 13 and 7 $\mu\text{mol DIP m}^{-2} \text{ h}^{-1}$, respectively) indicates that bottom and pore water supply similar amounts of DIP to *V. spiralis*. Sediments are often the main P source to macrophytes [58–60]. However, the relative importance of root and leaf uptake depends on the relative availability of DIP in pore and bottom waters. An empirical model suggests that the two P sources contribute similar amounts of DIP to macrophytes when the concentration ratio in pore and bottom water is 3.3:1.0 [61]. Above or below such a ratio, the sediment or the water column becomes a dominant P source.

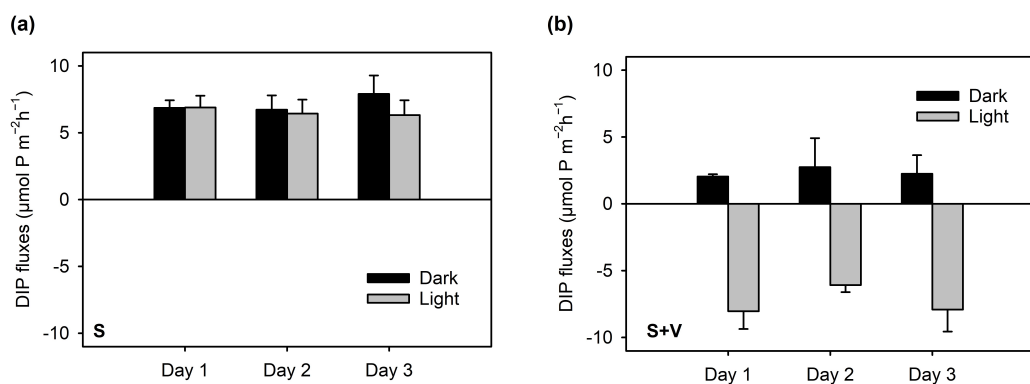


Figure 5. Light (gray bars) and dark (black bars) DIP fluxes measured in reconstructed microcosms containing bare sediment (S) (a) and bare sediment with transplanted individuals of *V. spiralis* (S + V) (b). Incubations were carried out over 3 different days. Averages \pm standard errors ($n = 6$) are reported.

3.4. Pore Water Features in Bare and Vegetated Sediments

The one-way analysis of variance revealed that pore water pH and ORP values and DIP, Fe^{2+} and Mn^{2+} concentrations measured in bare sediments (S) and sediments with transplanted *V. spiralis* (S + V) were all significantly different (Figure 6 and Table 2). In particular, the presence of *V. spiralis* resulted in lower pore water values of pH, DIP, and reduced Fe^{2+} and Mn^{2+} concentrations and in less negative ORP as compared to bare sediments. All these different parameters in the two treatments indicate a significant effect of the macrophyte roots in the organic-enriched sediments of the study area, likely due to a combination of radial oxygen loss, favoring aerobic processes and the oxidation of reduced chemical species, and assimilation of pore water solutes, reducing their concentration [42]. Lower pH in S + V treatment can be due to the release of exudates by the roots, stimulating heterotrophic microbial activity and CO_2 production [38,62].

The halved pore water concentration of DIP in S + V as compared to S results in a halved concentration gradient with bottom water and much lower DIP theoretical diffusive efflux. This agrees with the results of dark DIP fluxes in S that exceed by a factor of 3 dark DIP fluxes in S + V (Figure 5). Lower nutrient and chemically reduced species in vegetated than in bare sediments are widely reported in the literature [52,63,64].

In the present study, the pore water to bottom water ratio of DIP concentration in S + V was nearly 10:1. According to the empirical model of [61], this ratio would suggest a dominance of DIP uptake from *V. spiralis* roots, whereas from flux calculations, we speculated that nearly 50% of DIP uptake was from the leaves. However, in this study, DIP assimilation was estimated from measured oxygen fluxes using a conservative ROL value, which might lead, as already discussed, to underestimation. An increase in ROL would lead to an increase in net production and uptake, with the unaccounted P fraction being assimilated by sediment, adhering more closely to the model proposed by [61]. Another possible explanation could be the much lower DIP concentration in the proximity of root hair because, with Rhizon, an integrated water sample is collected, including sediment far from uptake zones.

Table 2. Results of the one-way analysis of variance on pore water features measured in the two treatments: bare sediments and sediments with *V. spiralis*. Significant values are printed in bold.

Parameter	Source of Variation	DF	SS	MS	F	p
pH	Between groups	1	0.210	0.210	46.722	<0.001
	Residual	8	0.0360	0.0045		
	Total	9	0.246			
ORP	Between groups	1	27,878.4	27,878.4	198.776	<0.001
	Residual	8	1122.0	140.25		
	Total	9	29,000.4			

Table 2. Cont.

Parameter	Source of Variation	DF	SS	MS	F	p
DIP	Between groups	1	2969.69	2968.69	637.736	<0.001
	Residual	8	37.253	4.657		
	Total	9	3006.943			
Fe^{2+}	Between groups	1	5326.652	5326.652	113.655	<0.001
	Residual	8	374.936	46.867		
	Total	9	5701.587			
Mn^{2+}	Between groups	1	29.872	29.872	126.319	<0.001
	Residual	8	1.892	0.236		
	Total	9	31.764			

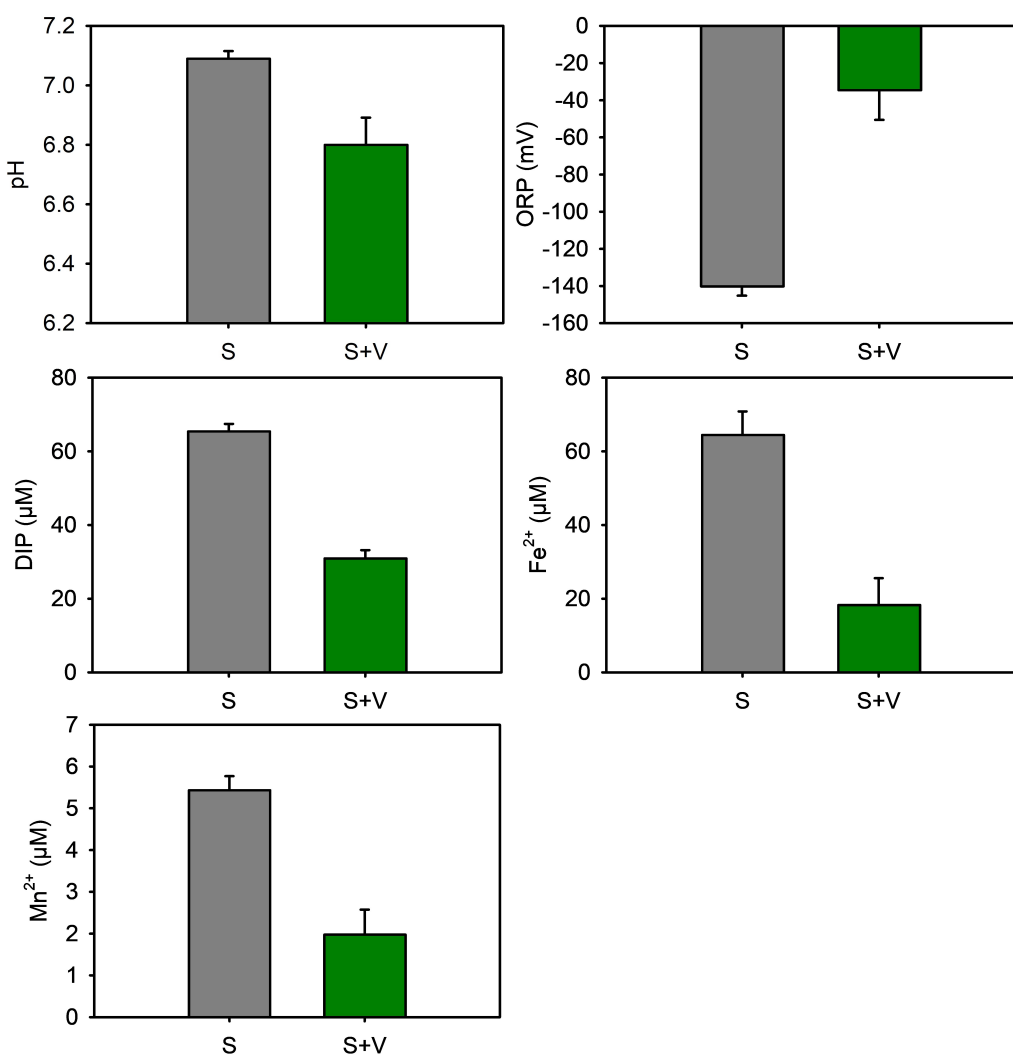


Figure 6. Comparison of pore water chemistry (pH, ORP, DIP, Fe^{2+} and Mn^{2+}) in bare sediments (S) and sediments with transplanted individuals of *V. spiralis* (S + V). pH and ORP were measured by inserting potentiometric electrodes in the microcosms, whereas DIP and Fe^{2+} and Mn^{2+} concentrations were measured in integrated pore water samples collected via Rhizon samplers vertically inserted in the central part of the microcosms.

3.5. Total P, Fe, and Mn within and on Roots

The graphs reported in the left column of Figure 7 show the results of total P, Fe, and Mn analyses carried out on the surface of *V. spiralis* roots (total P, Fe, and Mn precipitated or coprecipitated as plaques) and on the root ashes (total P, Fe, and Mn within the roots), along with increasing dry root biomass. The amount of the three elements increases linearly along with the root biomass both within and on the surface of the roots. However, the amount of P, Fe, and Mn on the root surface displayed a larger variability, likely due to the irregular distribution of plaques and to the different sediment horizons explored by the roots, characterized by different concentrations of solutes in the pore water [65]. The box plots in the right column of Figure 7 report the concentration of total P, Fe, and Mn within and on the roots of *V. spiralis* used in this experiment. The three elements always displayed higher concentrations on the roots than within the roots, by a factor of 2, 7, and 9 for P, Fe, and Mn, respectively. The median values of total P, Fe, and Mn were 102 and 215, 88 and 617, and 3.4 and 30.2 $\mu\text{mol g}_{\text{dw}}^{-1}$ within and on the root surface, respectively. Mn and Fe plaques were analyzed on the roots of different macrophytes (e.g., *Phragmites*

australis) where they occur as patchy, amorphous coatings [66]. Phosphorus and heavy metals were found to be adsorbed and immobilized on the surface of the Fe plaques, as demonstrated in the present study, but this did not reduce the macrophytes P content and growth rate [66–68]. P immobilization on the surface of roots can be compensated for by larger uptake of water column DIP by the leaves or contrasted by mechanisms of local acidification, solubilization, and uptake at the root level [69,70].

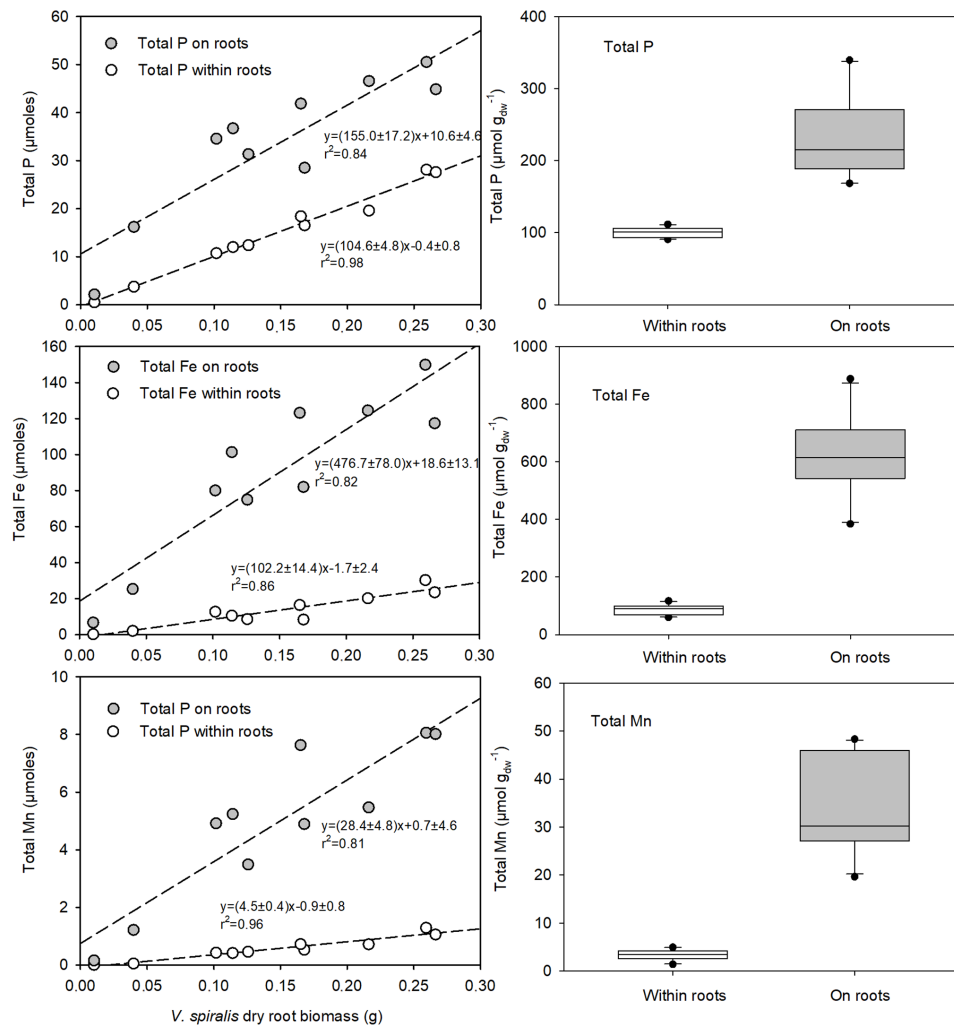


Figure 7. The panels on the left report the linear regressions between the amount of total P, Fe, and Mn present on the surface or within roots and the dry root biomass of *V. spiralis*. The panels on the right report the root biomass-normalized amount of total P, Fe, and Mn within and on roots. See the text for more details.

4. Conclusions

Results from this study suggest that submerged macrophytes releasing large amounts of O₂ via the roots perform an important indirect biogeochemical service as well as the direct uptake of solutes as they favor the precipitation of reduced metals as Fe²⁺ and Mn²⁺ and the coprecipitation of dissolved inorganic phosphorus on the root surface. This result aligns with results from pore water analyses, showing significantly lower concentrations of DIP, Fe²⁺ and Mn²⁺ in the presence of plants, and with results from fluxes, showing significantly lower dark DIP efflux in S + V. Implications of this indirect service are multiple, as the rhizosphere of *V. spiralis* can strongly reduce the concentration gradients between the pore and the bottom water, reducing the regenerative fluxes and the contribution of internal loads to eutrophication. Considering that the root biomass in a healthy meadow of *V. spiralis* can attain 40 g_{dw}m⁻², we speculate that 8.6, 24.7, and 1.2 mmol m⁻² of P, Fe,

and Mn can be retained within sediments, precipitated or coprecipitated on the roots. The transplant of a macrophyte with such high plasticity as *V. spiralis* can, therefore, represent an interesting nature-based solution to improve the chemical quality of sediments and of the water column, reducing the recycling of P. Other studies in the literature have focused on nitrogen and have revealed that *V. spiralis* performs an indirect biogeochemical service for this element by facilitating its loss via denitrification coupled to nitrification in the rhizosphere. By means of injection of $^{15}\text{NH}_4^+$ in the pore water, they demonstrated permanent N losses mediated by *V. spiralis* through ROL up to $100 \mu\text{mol N m}^{-2} \text{ h}^{-1}$ [40]. In the case of P, *V. spiralis* favors the immobilization of this element if the roots release part of the photosynthetically produced O₂ or acts as a conduit for bottom water O₂ [37].

The results of this study demonstrated that the success and remediation effectiveness of in situ transplants would depend on the maintenance of healthy meadows. The death of plants would likely result in metal reduction by microbial communities, stimulated by the large amount of root biomass, in the release of the coprecipitated P into the pore water and in its diffusion to the overlying water. The adaptability and survival capacity of the plants is influenced by multiple factors, including transparency and light availability, water depth and flow, bottom-up and top-down biological interactions, and, in highly polluted sites like the one under investigation, the long-term effects of multiple persistent pollutants [11]. To ensure the success of in situ applications, further investigations must concurrently address all these factors [71]. The survival of healthy meadows is closely connected to the reduction of external load. High nutrient concentration inhibits macrophyte growth, favoring opportunistic and fast-growing species [72]. The decrease in external loads enables tolerant macrophytes to modify the sediments, reducing internal loads and promoting oxidizing conditions. This, in turn, facilitates the recolonization of less-tolerant aquatic vegetation, establishing a chain of positive feedback for the ecosystem.

Author Contributions: Conceptualization, M.M., S.B., and M.B.; methodology, M.M., S.B., and M.B.; validation, M.M., S.B., and M.B.; investigation, M.M.; resources, M.B.; data curation, M.M.; writing—original draft preparation, M.M., S.B. and M.B.; writing—review and editing, M.M., S.B. and M.B.; supervision, M.B.; funding acquisition, M.B. All authors have read and agreed to the published version of the manuscript.

Funding: This research has financially been supported by the Program “FIL-Quota Incentivante” of University of Parma and co-sponsored by Fondazione Cariparma.

Data Availability Statement: Data can be accessed upon request to the corresponding author.

Acknowledgments: This work has benefited from the equipment and framework of the COMP-HUB and COMP-R Initiatives, funded by the “Departments of Excellence” program of the Italian Ministry for University and Research (MIUR, 2018–2022 and MUR, 2023–2027).

Conflicts of Interest: The authors declare no conflict of interest. The funders had no role in the design of the study, in the collection, analyses, or interpretation of data, in the writing of the manuscript, or in the decision to publish the results.

Abbreviations

The following abbreviations are used in this manuscript:

DIP	Dissolved Inorganic Phosphorus
DOU	Diffusive Oxygen Uptake
GPP	Gross Primary Production
NEM	Net Ecosystem Metabolism
NPP	Net Primary Production
OPD	Oxygen Penetration Depth
ROL	Radial Oxygen Loss

References

1. Nixon, S.W. Coastal marine eutrophication: A definition, social causes, and future concerns. *Ophelia* **1995**, *41*, 199–219. [[CrossRef](#)]
2. Nixon, S.W. Eutrophication and the macroscope. *Hydrobiologia* **2009**, *629*, 5–19. [[CrossRef](#)]

3. Fiskal, A.; Deng, L.; Michel, A.; Eickenbusch, P.; Han, X.; Lagostina, L.; Zhu, R.; Sander, M.; Schroth, M.H.; Bernasconi, S.M.; et al. Effects of eutrophication on sedimentary organic carbon cycling in five temperate lakes. *Biogeosciences* **2019**, *16*, 3725–3746. [[CrossRef](#)]
4. D’Angelo, E.M.; Reddy, K.R. Diagenesis of organic matter in a wetland receiving hypereutrophic Lake water: I. distribution of dissolved nutrients in the soil and water column. *J. Environ. Qual.* **1994**, *23*, 928–936. [[CrossRef](#)]
5. Phillips, G.; Bramwell’, A.; Pitt, J.; Stansfield, J.; Perrow, M. Practical application of 25 years’ research into the management of shallow lakes. *Hydrobiologia* **1999**, *395*, 61–76. [[CrossRef](#)]
6. Sas, H. *Lake Restoration by Reduction of Nutrient Loading: Expectations, Experiences, Extrapolations*; Academia Verlag: Berlin, Germany, 1989.
7. Conley, D.J.; Quigley, M.A.; Schelske, C.L. Silica and phosphorus flux from sediments: Importance of internal recycling in Lake Michigan. *Can. J. Fish. Aquat. Sci.* **1988**, *45*, 1030–1035. [[CrossRef](#)]
8. Tay, C.J.; Koh, H.L.; Mohd, M.H.; Teh, S.Y. Assessing the role of internal phosphorus recycling on eutrophication in four lakes in China and Malaysia. *Ecol. Inform.* **2022**, *72*, 101830. [[CrossRef](#)]
9. Anderson, H.S.; Johengen, T.H.; Miller, R.; Godwin, C.M. Accelerated sediment phosphorus release in Lake Erie’s central basin during seasonal anoxia. *Limnol. Oceanogr.* **2021**, *66*, 3582–3595. [[CrossRef](#)]
10. Mucci, M.; Maliaka, V.; Noyma, N.P.; Marinho, M.M.; Lürling, M. Assessment of possible solid-phase phosphate sorbents to mitigate eutrophication: Influence of pH and anoxia. *Sci. Total Environ.* **2018**, *619*, 619–620, 1431–1440. [[CrossRef](#)]
11. Wang, D.; Gan, X.; Wang, Z.; Jiang, S.; Zheng, X.; Zhao, M.; Zhang, Y.; Fan, C.; Wu, S.; Du, L. Research status on remediation of eutrophic water by submerged macrophytes: A review. *Process. Saf. Environ. Prot.* **2023**, *169*, 671–684. [[CrossRef](#)]
12. Li, Y.; Wang, L.; Yan, Z.; Chao, C.; Yu, H.; Yu, D.; Liu, C. Effectiveness of dredging on internal phosphorus loading in a typical aquacultural lake. *Sci. Total Environ.* **2020**, *744*, 140883. [[CrossRef](#)]
13. Zamparas, M.; Zacharias, I. Restoration of eutrophic freshwater by managing internal nutrient loads. A review. *Sci. Total Environ.* **2014**, *496*, 551–562. [[CrossRef](#)]
14. Knopik, J.M.; Newman, R.M. Transplanting aquatic macrophytes to restore the littoral community of a eutrophic lake after the removal of common carp. *Lake Reserv. Manag.* **2018**, *34*, 365–375. [[CrossRef](#)]
15. Barko, J.W.; Smart, R.M. Sediment-Related Mechanisms of Growth Limitation in Submersed Macrophytes. *Ecology* **1986**, *67*, 1328–1340. [[CrossRef](#)]
16. Egertson, C.J.; Kopaska, J.A.; Downing, J.A. A century of change in macrophyte abundance and composition in response to agricultural eutrophication. *Hydrobiologia* **2004**, *524*, 145–156. [[CrossRef](#)]
17. Geurts, J.J.; Sarneel, J.M.; Willers, B.J.; Roelofs, J.G.; Verhoeven, J.T.; Lamers, L.P. Interacting effects of sulphate pollution, sulphide toxicity and eutrophication on vegetation development in fens: A mesocosm experiment. *Environ. Pollut.* **2009**, *157*, 2072–2081. [[CrossRef](#)] [[PubMed](#)]
18. Terrados, J.; Duarte, C.; Kamp-Nielsen, L.; Agawin, N.; Gacia, E.; Lacap, D.; Borum, J.; Lubanski, M.; Greve, T. Are seagrass growth and survival constrained by the reducing conditions of the sediment? *Aquat. Bot.* **1999**, *65*, 175–197. [[CrossRef](#)]
19. Sand-Jensen, K.; Borum, J.; Binzer, T. Oxygen stress and reduced growth of *Lobelia dortmanna* in sandy lake sediments subject to organic enrichment. *Freshw. Biol.* **2005**, *50*, 1034–1048. [[CrossRef](#)]
20. Preiner, S.; Dai, Y.; Pucher, M.; Reitsema, R.E.; Schoelynck, J.; Meire, P.; Hein, T. Effects of macrophytes on ecosystem metabolism and net nutrient uptake in a groundwater fed lowland river. *Sci. Total Environ.* **2020**, *721*, 137620. [[CrossRef](#)]
21. Wu, L.; Kellogg, L.; Devol, A.H.; Tiedje, J.M.; Zhou, J. Microarray-based characterization of microbial community functional structure and heterogeneity in marine sediments from the Gulf of Mexico. *Appl. Environ. Microbiol.* **2008**, *74*, 4516–4529. [[CrossRef](#)]
22. Xue, L.; Ren, H.; Li, S.; Leng, X.; Yao, X. Soil bacterial community structure and co-occurrence pattern during vegetation restoration in karst rocky desertification area. *Front. Microbiol.* **2017**, *8*, 2377. [[CrossRef](#)]
23. Lemoine, D.G.; Mermilliod-Blondin, F.; Barrat-Segretain, M.H.; Massé, C.; Malet, E. The ability of aquatic macrophytes to increase root porosity and radial oxygen loss determines their resistance to sediment anoxia. *Aquat. Ecol.* **2012**, *46*, 191–200. [[CrossRef](#)]
24. Fritioff, A.; Kautsky, L.; Greger, M. Influence of temperature and salinity on heavy metal uptake by submersed plants. *Environ. Pollut.* **2005**, *133*, 265–274. [[CrossRef](#)] [[PubMed](#)]
25. Jackson, L.J. Paradigms of metal accumulation in rooted aquatic vascular plants. *Sci. Total Environ.* **1998**, *219*, 223–231. [[CrossRef](#)]
26. Marchand, L.; Mench, M.; Jacob, D.L.; Otte, M.L. Metal and metalloid removal in constructed wetlands, with emphasis on the importance of plants and standardized measurements: A review. *Environ. Pollut.* **2010**, *158*, 3447–3461. [[CrossRef](#)] [[PubMed](#)]
27. Brix, H. Do macrophytes play a role in constructed treatment wetlands? *Water Sci. Technol.* **1997**, *35*, 11–17. [[CrossRef](#)]
28. Human, L.R.; Snow, G.C.; Adams, J.B.; Bate, G.C.; Yang, S.C. The role of submerged macrophytes and macroalgae in nutrient cycling: A budget approach. *Estuar. Coast. Shelf Sci.* **2015**, *154*, 169–178. [[CrossRef](#)]
29. Malec, P.; Mysliwa-Kurdziel, B.; Prasad, M.N.V.; Waloszek, A.; Strzałka, K. Role of aquatic macrophytes in biogeochemical cycling of heavy metals, relevance to soil-sediment continuum detoxification and ecosystem health. In *Detoxification of Heavy Metals*; Springer: Berlin/Heidelberg, Germany, 2011; pp. 345–368. [[CrossRef](#)]
30. Cronk, J.K.; Fennessy, M.S. *Wetland Plants: Biology and Ecology*; CRC Press: Boca Raton, FL, USA, 2016.
31. Wigand, C.; Wehr, J.; Limburg, K.; Gorham, B.; Longergan, S.; Findlay, S. Effect of *Vallisneria americana* (L.) on community structure and ecosystem function in lake mesocosms. *Hydrobiologia* **2000**, *418*, 137–146. [[CrossRef](#)]

32. Les, D.H.; Jacobs, S.W.L.; Tippery, N.P.; Chen, L.; Moody, M.L.; Wilstermann-Hildebrand, M. Systematics of *Vallisneria* (Hydrocharitaceae). *Syst. Bot.* **2008**, *33*, 49–65. [[CrossRef](#)]
33. Soana, E.; Naldi, M.; Bonaglia, S.; Racchetti, E.; Castaldelli, G.; Brüchert, V.; Viaroli, P.; Bartoli, M. Benthic nitrogen metabolism in a macrophyte meadow (*Vallisneria spiralis* L.) under increasing sedimentary organic matter loads. *Biogeochemistry* **2015**, *124*, 387–404. [[CrossRef](#)]
34. Wang, J.; Yu, D. Influence of sediment fertility on morphological variability of *Vallisneria spiralis* L. *Aquat. Bot.* **2007**, *87*, 127–133. [[CrossRef](#)]
35. Xie, Y.; An, S.; Yao, X.; Xiao, K.; Zhang, C. Short-time response in root morphology of *Vallisneria natans* to sediment type and water-column nutrient. *Aquat. Bot.* **2005**, *81*, 85–96. [[CrossRef](#)]
36. Yan, Z.S.; Guo, H.Y.; Song, T.S.; Hu, Y.; Jiang, H.L. Tolerance and remedial function of rooted submersed macrophyte *Vallisneria spiralis* to phenanthrene in freshwater sediments. *Ecol. Eng.* **2011**, *37*, 123–127. [[CrossRef](#)]
37. Marzocchi, U.; Benelli, S.; Larsen, M.; Bartoli, M.; Glud, R.N. Spatial heterogeneity and short-term oxygen dynamics in the rhizosphere of *Vallisneria spiralis*: Implications for nutrient cycling. *Freshw. Biol.* **2019**, *64*, 532–543. [[CrossRef](#)]
38. Soana, E.; Bartoli, M. Seasonal variation of radial oxygen loss in *Vallisneria spiralis* L.: An adaptive response to sediment redox? *Aquat. Bot.* **2013**, *104*, 228–232. [[CrossRef](#)]
39. Pinardi, M.; Bartoli, M.; Longhi, D.; Marzocchi, U.; Laini, A.; Ribaudo, C.; Viaroli, P. Benthic metabolism and denitrification in a river reach: A comparison between vegetated and bare sediments. *J. Limnol.* **2009**, *68*, 133–145. [[CrossRef](#)]
40. Racchetti, E.; Longhi, D.; Ribaudo, C.; Soana, E.; Bartoli, M. Nitrogen uptake and coupled nitrification-denitrification in riverine sediments with benthic microalgae and rooted macrophytes. *Aquat. Sci.* **2017**, *79*, 487–505. [[CrossRef](#)]
41. Hupfer, M.; Dollan, A. Immobilisation of phosphorus by iron-coated roots of submerged macrophytes. *Hydrobiologia* **2003**, *506–509*, 635–640. [[CrossRef](#)]
42. Han, C.; Ren, J.; Wang, Z.; Yang, S.; Ke, F.; Xu, D.; Xie, X. Characterization of phosphorus availability in response to radial oxygen losses in the rhizosphere of *Vallisneria spiralis*. *Chemosphere* **2018**, *208*, 740–748. [[CrossRef](#)]
43. Stocum, E.T.; Plante, C.J. The effect of artificial defaunation on bacterial assemblages of intertidal sediments. *J. Exp. Mar. Biol. Ecol.* **2006**, *337*, 147–158. [[CrossRef](#)]
44. Dalsgaard, T.; Nielsen, L.P.; Brotas, V.; Viaroli, P.; Underwood, G.J.C.; Nedwell, D.B.; Sundback, K.; Rysgaard, S.; Miles, A.; Bartoli, M.; et al. *Protocol Handbook for NICE-Nitrogen Cycling in Estuaries: A Project under the EU Research Programme: Marine Science and Technology (MAST III)*; Department of Lake and Estuarine Ecology, Ministry of Environment and Energy National Environmental Research Institute: Silkeborg, Denmark, 2000.
45. APHA. *Standard Methods for the Examination of Water and Wastewaters*, 18th ed.; APHA: Washington, DC, USA; New York, NY, USA, 1992.
46. Valderrama, J.C. *Methods Used by the Hydrographic Department of the National Board of Fisheries*; Grasshoff, K., Ed.; Interim Commission for the Protection of the Environment of the Baltic Sea: Goteborg, Sweden, 1977.
47. Bartoli, M.; Longhi, D.; Nizzoli, D.; Como, S.; Magni, P.; Viaroli, P. Short term effects of hypoxia and bioturbation on solute fluxes, denitrification and buffering capacity in a shallow dystrophic pond. *J. Exp. Mar. Biol. Ecol.* **2009**, *381*, 105–113. [[CrossRef](#)]
48. Rasmussen, H.; Jørgensen, B.B. Microelectrode studies of seasonal oxygen uptake in a coastal sediment: Role of molecular. *Mar. Ecol. Prog. Ser.* **1992**, *81*, 289–303. [[CrossRef](#)]
49. Nielsen, L.P.; Christensen, P.B.; Revsbech, N.P.; Sørensen, J. Denitrification and oxygen respiration in biofilms studied with a microsensor for nitrous oxide and oxygen. *Microb. Ecol.* **1990**, *19*, 63–72. [[CrossRef](#)] [[PubMed](#)]
50. Ruttenberg, C. Development of a sequential extraction method for different forms of phosphorus in marine sediments. *Limnol. Oceanogr.* **1992**, *37*, 1460–1482. [[CrossRef](#)]
51. Aspila, K.I.; Agemian, H.; Chau, A.S. A semi-automated method for the determination of inorganic, organic and total phosphate in sediments. *Analyst* **1976**, *101*, 187–197. [[CrossRef](#)] [[PubMed](#)]
52. Ribaudo, C.; Bartoli, M.; Racchetti, E.; Longhi, D.; Viaroli, P. Seasonal fluxes of O₂, DIC and CH₄ in sediments with *Vallisneria spiralis*: Indications for radial oxygen loss. *Aquat. Bot.* **2011**, *94*, 134–142. [[CrossRef](#)]
53. Caffrey, J.M.; Kemp, W.M. Seasonal and spatial patterns of oxygen production, respiration and root-rhizome release in *Potamogeton perfoliatus* L. and *Zostera marina* L. *Aquat. Bot.* **1991**, *40*, 109–128. [[CrossRef](#)]
54. Colmer, T.D. Long-distance transport of gases in plants: A perspective on internal aeration and radial oxygen loss from roots. *Plant Cell Environ.* **2003**, *26*, 17–36. [[CrossRef](#)]
55. Pezeshki, S.R. Wetland plant responses to soil flooding. *Environ. Exp. Bot.* **2001**, *46*, 299–312. [[CrossRef](#)]
56. Aldridge, K.T.; Ganf, G.G. Modification of sediment redox potential by three contrasting macrophytes: Implications for phosphorus adsorption/desorption. *Mar. Freshw. Res.* **2003**, *54*, 87–94. [[CrossRef](#)]
57. Delgard, M.L.; Deflandre, B.; Bernard, G.; Richard, M.; Kochoni, E.; Charbonnier, C.; Cesbron, F.; Metzger, E.; Grémare, A.; Anschutz, P. Benthic oxygen exchange over a heterogeneous *Zostera noltei* meadow in a temperate coastal ecosystem. *Mar. Ecol. Prog. Ser.* **2016**, *543*, 55–71. [[CrossRef](#)]
58. Barko, J.W.; Michael, R. Mobilization of sediment phosphorus by submersed freshwater macrophytes. *Freshw. Biol.* **1980**, *10*, 229–238. [[CrossRef](#)]
59. Carignan, R.; Kalff, J. Phosphorus sources for aquatic weeds: Water or sediments? *Science* **1980**, *29*, 987–989. [[CrossRef](#)] [[PubMed](#)]

60. Rattray, M.R.; Howard-Williams, C.; Brown, J.M.A. Sediment and water as sources of nitrogen and phosphorus for submerged rooted aquatic macrophytes. *Aquat. Bot.* **1991**, *40*, 225–237. [[CrossRef](#)]
61. Carignan, R. An empirical model to estimate the relative importance of roots in phosphorus uptake by aquatic macrophytes. *Can. J. Fish. Aquat. Sci.* **1982**, *39*, 243–247. [[CrossRef](#)]
62. Gao, Y.N.; Liu, B.Y.; Xu, D.; Zhou, Q.H.; Hu, C.Y.; Ge, F.J.; Zhang, L.P.; Wu, Z.B. Introduction phenolic compounds exuded from two submerged freshwater macrophytes and their allelopathic effects on microcystis aeruginosa. *Pol. J. Environ. Stud.* **2011**, *20*, 1153–1159.
63. Soana, E.; Naldi, M.; Bartoli, M. Effects of increasing organic matter loads on pore water features of vegetated (*Vallisneria spiralis* L.) and plant-free sediments. *Ecol. Eng.* **2012**, *47*, 141–145. [[CrossRef](#)]
64. Wigand, C.; Finn, M.; Findlay, S.; Fischer, D. Submersed macrophyte effects on nutrient exchanges in riverine sediments. *Estuaries* **2001**, *24*, 398–406. [[CrossRef](#)]
65. Laskov, C.; Herzog, C.; Lewandowski, J.; Hupfer, M. Miniaturized photometrical methods for the rapid analysis of phosphate, ammonium, ferrous iron, and sulfate in pore water of freshwater sediments. *Limnol. Oceanogr. Methods* **2007**, *4*, 63–71. [[CrossRef](#)]
66. Batty, L.C.; Baker, A.J.; Wheeler, B.D. Aluminium and phosphate uptake by *Phragmites australis*: The role of Fe, Mn and Al root plaques. *Ann. Bot.* **2002**, *89*, 443–449. [[CrossRef](#)]
67. Jiang, F.Y.; Chen, X.; Luo, A.C. Iron plaque formation on wetland plants and its influence on phosphorus, calcium and metal uptake. *Aquat. Ecol.* **2009**, *43*, 879–890. [[CrossRef](#)]
68. Zandi, P.; Yang, J.; Darma, A.; Bloem, E.; Xia, X.; Wang, Y.; Li, Q.; Schnug, E. Iron plaque formation, characteristics, and its role as a barrier and/or facilitator to heavy metal uptake in hydrophyte rice (*Oryza sativa* L.). *Environ. Geochem. Health* **2023**, *45*, 525–559. [[CrossRef](#)] [[PubMed](#)]
69. Brodersen, K.E.; Koren, K.; Moßhammer, M.; Ralph, P.J.; Kühl, M.; Santner, J. Seagrass-mediated phosphorus and iron solubilization in tropical sediments. *Environ. Sci. Technol.* **2017**, *51*, 14155–14163. [[CrossRef](#)] [[PubMed](#)]
70. Xing, X.; Ding, S.; Liu, L.; Chen, M.; Yan, W.; Zhao, L.; Zhang, C. Direct evidence for the enhanced acquisition of phosphorus in the rhizosphere of aquatic plants: A case study on *Vallisneria natans*. *Sci. Total Environ.* **2018**, *616–617*, 386–396. [[CrossRef](#)]
71. Li, Y.; Wang, L.; Chao, C.; Yu, H.; Yu, D.; Liu, C. Submerged macrophytes successfully restored a subtropical aquacultural lake by controlling its internal phosphorus loading. *Environ. Pollut.* **2021**, *268*, 115949. [[CrossRef](#)]
72. Ozimek, T.; Kowalczewski, A. Long-term changes of the submerged macrophytes in eutrophic Lake Mikolajskie (Poland). *Aquat. Bot.* **1984**, *19*, 1–11. [[CrossRef](#)]

Disclaimer/Publisher’s Note: The statements, opinions and data contained in all publications are solely those of the individual author(s) and contributor(s) and not of MDPI and/or the editor(s). MDPI and/or the editor(s) disclaim responsibility for any injury to people or property resulting from any ideas, methods, instructions or products referred to in the content.